

# Structural setting of Iron oxide-apatite and Fe-Cu-sulphide occurrences in Kiruna, Northern Sweden: *Complementary material*

Joel BH Andersson\*, Leslie Logan, Tobias E Bauer, and Olof Martinsson

Division of Geosciences and Environmental Engineering, Luleå University of Technology, SE-971 87 Luleå, Sweden

\* Corresponding author: joel.bh.andersson@ltu.se; +46 73 0821280



## Background

The Norrbotten lithotectonic unit (Stephens 2020) in northern Sweden hosts numerous iron and base metal deposits (Fig. 1), whereof the world-class Kiirunavaara iron oxide-apatite (IOA) deposit is the most famous one. The area shares many geological characteristics to other IOA and iron oxide-Cu-Au (IOCG) prospective terrains around the world. Similarities include a variable distributed sodic and potassic alteration, bimodal character of host volcanic rocks, and the deposits tend to be either hosted by, or spatially related, to crustal scale deformation zones. Despite of the common structural control on mineralized systems in Norrbotten, only few studies have been performed focusing on the linkage between deformation, mineralization, and hydrothermal alteration. In this predominantly field-based project, we focus on the structural setting and evolution in Kiruna (Fig. 1) and the relation to iron oxide-apatite, Fe-Cu-sulphide and their associated hydrothermal alteration.

This complementary material to the EGU-abstract number EGU-2020-280 aims at providing an overview of the most recent geological research produced within the CAMM (Centre of Advanced Mining and Metallurgy)-project as well as preliminary results from the Horizon 2020 project “New Exploration Technologies (NEXT)” at the Luleå University of Technology. We use results published in Andersson (2019), Andersson et al. (2019, 2020), as well as new material in order to set these studies in a broader perspective.

## Stratigraphy

The Kiruna area constitutes the best-preserved continuous Rhyacian-Orosirian stratigraphic sequence in the Norrbotten region. The supracrustal pile is dipping and younging towards east. The Orosirian Kurravaara conglomerate marks the stratigraphic lowest unit and is (Fig. 2A), interpreted as an alluvial fan deposit (Kumpulainen 2000) overlying Rhyacian basaltic pillow lavas. Stratigraphically above the Kurravaara conglomerate, volcanic and volcanoclastic rocks host the largely concordant Kiirunavaara and Loussavaara IOA deposits at the contact between basaltic-andesitic rocks (Hopukka formation; 2B) and rhyodacitic rocks (Loussavaara formation; 2C, D). A stratigraphically higher, and largely concordant, horizon of IOA-miner-

alization is present between the Loussavaara formation (Fig. 2C, D) and ignimbritic rhyolite (Frietsch 1979) of the Matojärvi formation (Fig. 2E). The Matojärvi formation is a heterogeneous and highly tectonized unit of ignimbritic rhyolite (2E), basaltic agglomerate and tuff (Fig. 2F), breccia-conglomerate (Fig. 2G), greywacke (Fig. 2H), and phyllite (Fig. 2I). The uppermost unit, the Hauki quartzite, marks the end of the Orosirian in the Kiruna area and constitutes cross-bedded quartz-arenite (Fig. 2J) interrupted by breccia-conglomerate in a lower (Fig. 2K) and an upper horizon (Fig. 2L). The volcanic rocks, as well as the ores, were deposited during a short time interval of approx. 15 M. y. (Westhues et al. 2016).

## Structural geology and tectonic interpretation

The stratigraphic column (Fig. 2M) indicates basin development during the emplacement of the IOA deposits in Kiruna. During subsequent compression (D1-D2), the basin was inverted. During D1 a heterogeneously developed continuous S1 cleavage was distributed regionally and shear zones were localized at lithological contacts and favorable volcanoclastic and sedimentary rocks. The same structures were largely re-activated with differing kinematics under more brittle conditions during D2 (Andersson et al. 2020). No regionally distributed cleavage was produced during D2, instead F2 folds in low strain blocks adjacent to shear zones tend to lack axial planar cleavage and when present it is spaced and brittle. West of Kiruna, the shear zones show reverse oblique (D1; Fig. 3A) and reverse dip-slip (D2; Fig. 3B) with an overall west-side-up sense-of-shear (Andersson et al. 2020). Contrasting kinematics are shown by the shear zones in Kiruna where reverse oblique and reverse dip-slip movements (D2; Fig. 3C, D) give an overall east-side-up sense-of-shear (Andersson 2019). Brittle components are uncommon in D1-structures whereas brittle and plastic structures formed simultaneous during D2 both in Kiruna (Fig. 3E) and regionally to the west (Fig. 3F; Andersson et al. 2020) indicating higher crustal levels during D2. The contrasting kinematics from west to east results in reverse west-dipping shear zones to the west, and reverse east-dipping shear zones to the east (cf. Fig. 4, 5). The result is a juxtaposition of different crustal levels with a central block of lower metamorphic grade (central Kiruna) surrounded by rocks of higher metamorphic grade.

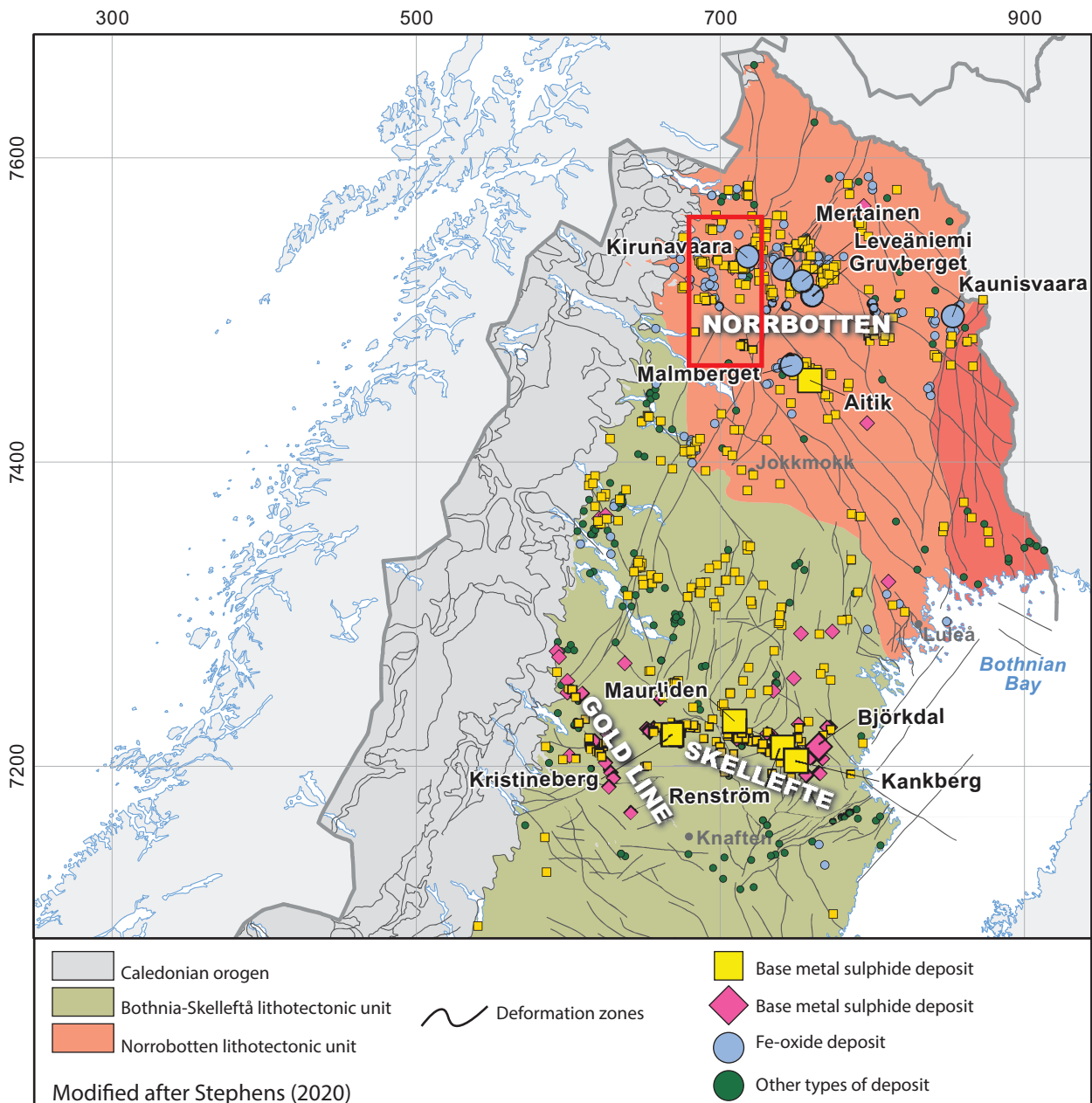


**Figure 1: Geological map modified after Stephens (2020).**

### Hydrothermal alteration

The hydrothermal alteration linked to D1 is comprised of scapolite  $\pm$  albite  $\pm$  sulphide that formed coeval with a magnetite + amphibole alteration (Fig. 6A; Andersson et al. 2020). In thin section, annealed pyrite textures and porous rim-growth with albite inclusions indicate pyrite recrystallization occurred after albitization and synchronous with magnetite-actinolite alteration during D1 (Fig. 6B). The alteration styles characteristic for the D2-event is more diverse and potassic-ferroan in character and most often hosted by D2-structures. It is comprised of K-feldspar  $\pm$  epidote  $\pm$  quartz  $\pm$  biotite  $\pm$  magnetite  $\pm$  sericite associated to Fe- and Cu-sulphide (Fig. 6C; Andersson et al. 2020). Both brittle and ductile D2-structures constitute effective traps for sulphide. Figure 6D shows a drill core sample of a F2-folded sequence in a phyllite horizon of the Matojärvi formation. X-ray computed tomography imaging in combination with continuous XRF-scanning of the same drill core sample reveal that pyrite was transported along brittle axial planar S2 and trapped in the F2 hinge zone (Fig. 6E; Andersson et al. 2019).

### Discussion

Two major deformation events in northern Norrbotten are frequently reported regionally (e.g. Bergman et al. 2001, Bauer 2018, Bergman 2018, Andersson 2019). The timing of these deformation events is poorly constrained but thought to overlap with early and late syn-orogenic magmatism at c. 1.88 Ga and c. 1.78 Ga (Bergman et al. 2001, Sarlus et al. 2017) respectively. Ore formation associated to early magmatism comprises both IOA and IOCG formation even though geochronological data indicate that IOA emplacement is marginally earlier than IOCG during this early tectono-magmatic event (cf. Romer et al. 1994, Smith et al. 2009, Martinsson et al. 2016, Westheus et al. 2016). On the other hand, ore formation linked to late magmatism is dominated by structurally controlled IOCG deposits hosted by D2 structures and it is likely that these ores represent remobilization of earlier and more significant base metal deposits.

The significance of the sulphide remobilization-entrapment in cm-scale linked to D2-deformation in this study is ambiguous. However, we believe these small-scale key-observations will help understand regional scale remobilization-entrapment mechanisms linked to D2-deformation northern Norrbotten.





HIGH STRAIN	Arenite	Hauki Quartzite
	Breccia-Conglomerate	
	Arenite	Matojärvi formation
	Breccia-Conglomerate	
	Phyllite	
	Greywacke	
	Breccia-conglomerate	
	Basaltic lava, tuff, agglomerate	Luossavaara formation
	Rhyolite tuff, ignimbrite	
	Rhyodacitic tuff, coherent volcanic, breccia conglomerate	
	Basaltic, trachyandesitic sub-volcanic and lavas	Hopukka formation
	Conglomerate	Kurravaara conglomerate
	Greywacke	
	Conglomerate	

M

**Figure 2: Field images showing key localities of the Orosirian part of the stratigraphy. From bottom: A) Breccia-conglomerate of the Kurravaara conglomerate. B) Basalt-andesite of the Hopukka formation. C) Rhyodacite of the Loussavaara formation. D) Breccia-conglomerate of the Loussavaara formation. E) K-feldspar altered rhyolite of the Matojärvi formation. F) Basaltic agglomerate of the Matojärvi formation. G) Breccia-conglomerate of the Matojärvi formation. H) Graywacke of the Matojärvi formation. I) Phyllite of the Matojärvi formation. J) Cross-bedded quartz-arenite of the Hauki quartzite. K) Lower conglomerate of the Hauki quartzite. L) Upper conglomerate of the Hauki quartzite. M) Stratigraphic column of the Kiruna area showing the Orosirian part of the stratigraphy.**



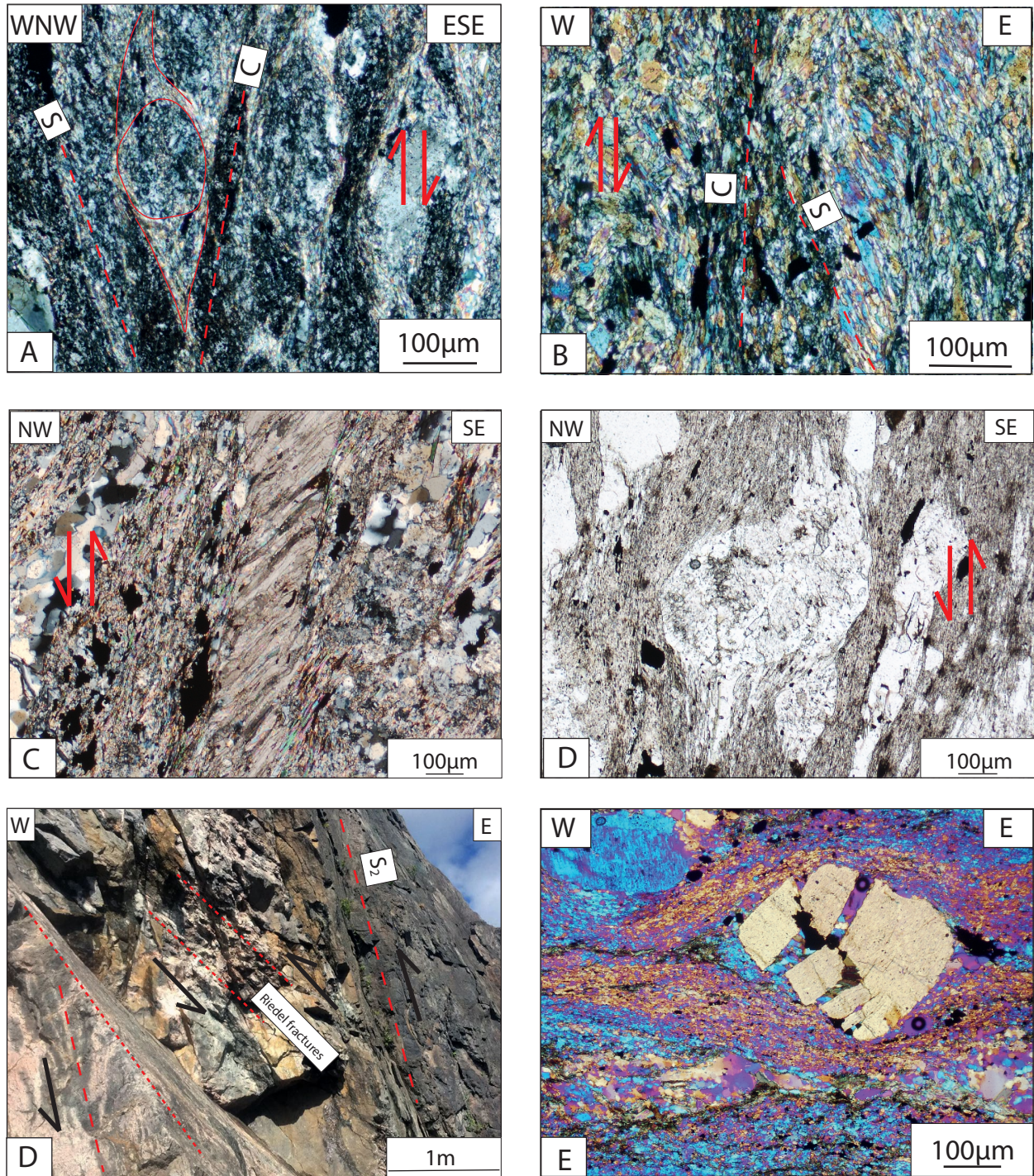


**Figure 3** Kinematic indications of microstructures and of a field locality. *A)* Asymmetric sigmoid and SC-fabric indicating west-side-up, west of central Kiruna, Andersson et al. (2020). *B)* SC-fabric indicating west-side-up, west of central Kiruna, Andersson et al. (2020). *C)* Oblique foliation in a calcite domain indicating east-side-up, central Kiruna. *D)* Asymmetric sigma-clast indicating east-side-up, central Kiruna. *E)* Riedel shear fractures developed in competent volcanic rocks indicating east-side-up. Ductile shearing at ore contact, central Kiruna. *F)* Brittle fracturing of feldspar in a dynamically recrystallized quartz matrix.



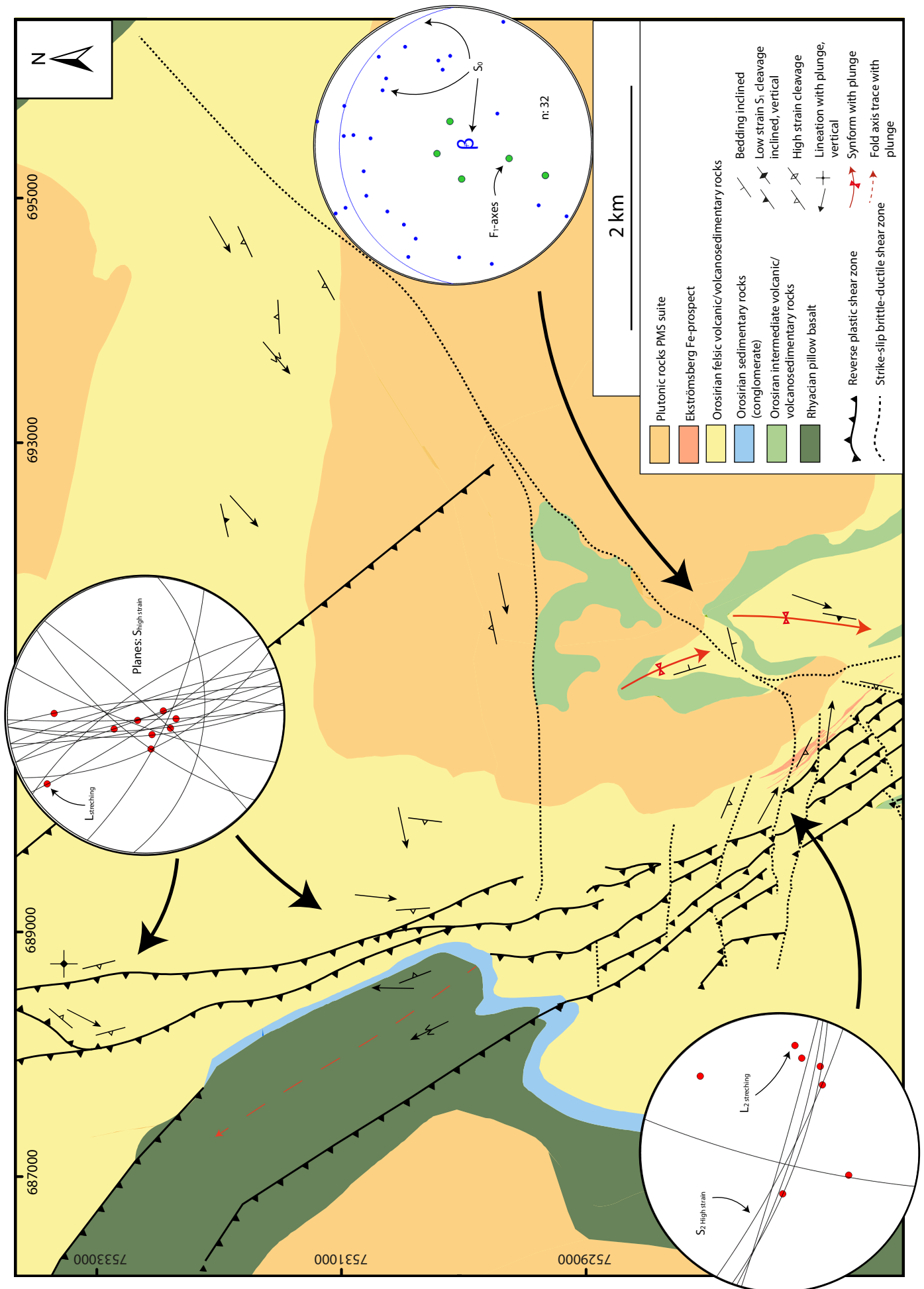


Figure 4 Geological map of the Ekströmsberg area, west of Kiruna (Andersson et al 2020). The map shows steep west-dipping reverse shear zones sub-parallel with the shear zones in central Kiruna.



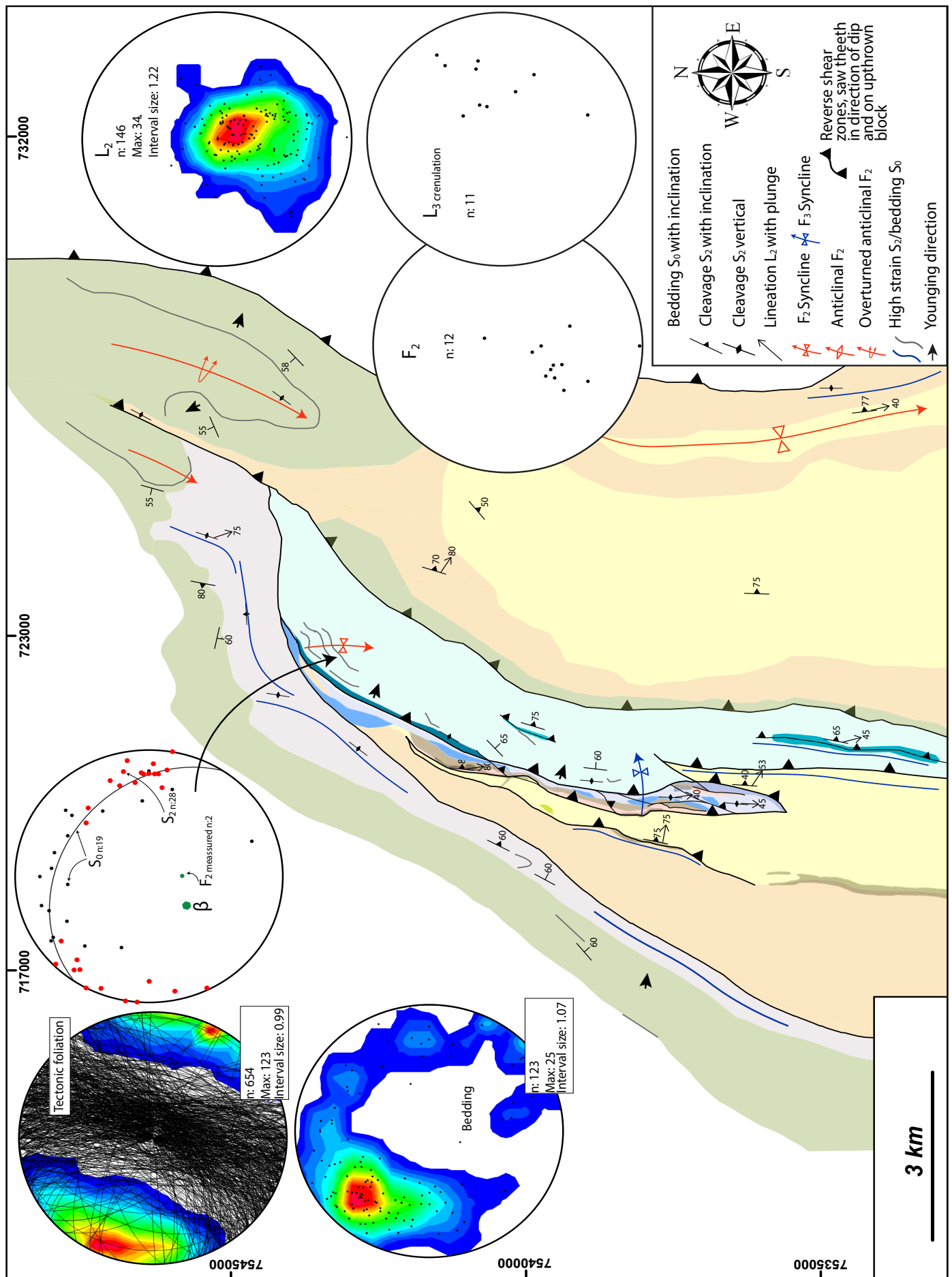
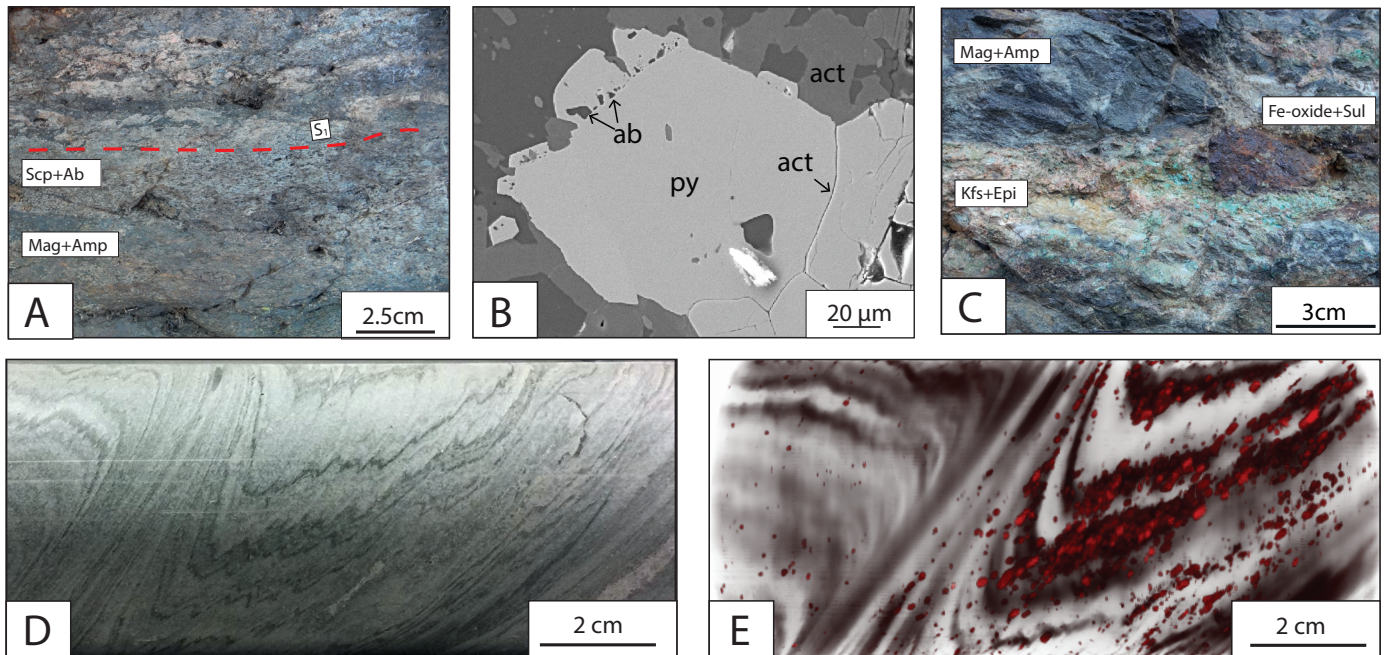


Figure 5 Structural map of the central Kiruna area. The map shows steep east-dipping reverse shear zones.





**Figure 6** Hydrothermal alteration, A, C from Andersson et al. (2020), D-E from Andersson et al. (2019). A) Magnetite + amphibole alteration overprinted by scapolite + albite alteration, broadly D1-timing. B) BSE imaging of annealed pyrite recrystallized in an albite + pyrite + magnetite + actinolite mineral association C) K-feldspar + epidote + Fe-oxide + sulphide alteration of D2-timing overprinting magnetite + amphibole alteration. D) Drill core section showing an antithetic flank fold in phyllite. E) CT-image of the same fold as in Fig. 6D. Red: pyrite, black: chlorite, dark grey: chlorite + white mica + quartz, light grey: white mica + quartz.

### Acknowledgement

This study was financed by Centre of Advanced Mining and Metallurgy (Camm). Loussavaara-Kiirunavaara AB is thanked for supporting the project.

### References

- Andersson, J. B. H.: Structural evolution of two ore-bearing Palaeoproterozoic metasupracrustal belts in the Kiruna area, northwestern Fennoscandian Shield, Licentiate thesis, Luleå University of Technology, 28pp, 2019.
- Andersson, J. B. H., Warlo, M., Bauer, T. E., Bergqvist, M., and Hansson, A.: Structural controls on sulphide (re)-distribution in Kiruna, Abstract volume, SGA biennial meeting 2019, Glasgow, August, 115-118, 2019.
- Andersson, J. B. H., Bauer, T. E., and Lynch, E. P.: Evolution of structures and hydrothermal alteration in a Palaeoproterozoic supracrustal belt: Constraining paired deformation-fluid flow events in an Fe and Cu-Au prospective terrain in northern Sweden, *Solid Earth*, 11, 547-578, 2020.
- Bauer, T. E., Andersson, J. B. H., Sarlus, Z., Lund, C., and Kearney, T.: Structural controls on the setting, shape, and hydrothermal alteration of the Malmberget iron oxide-apatite deposit, Northern Sweden, *Econ. Geol.*, 113, 377-395, 2018.
- Bergman, S., Kübler, L., and Martinsson, O.: Description of regional geological and geophysical maps of northern Norrbotten County (east of the Caledonian orogen), *Geol. Surv. of Swe.*, Ba56, 110 pp., 2001.
- Bergman, S.: Geology of the northern Norrbotten ore province, northern Sweden, *Rapporter och Meddelanden 141*, *Geol. Surv. of Swe.*, Uppsala, 428 pp., 2018.
- Frietsch, R.: Petrology of the Kurravaara area, northeast of Kiruna, northern Sweden. *Geol. Surv. of Swe.*, C760, 82p., 1979.
- Martinsson, O., Billström, K., Broman, C., Weihed, P., and Wanhainen, C.: Metallogeny of the Northern Norrbotten Ore Province, Northern Fennoscandian Shield with emphasis on IOCG and apatite-iron ore deposits, *Ore Geol. Rev.*, 78, 447-492, 2016.
- Kumpulainen, R. A.: The Palaeoproterozoic sedimentary record of northernmost Norrbotten, Sweden. *Geol. Surv. of Swe*, unpublished report, BRAP 200030, 45 pp. 2000.
- Romer, R., Martinsson, O., and Perdahl, J.-A.: Geochronology of the Kiruna iron ores and related hydrothermal alteration, *Econ. Geol.*, 89, 1249-1261, 1994.
- Sarlus, Z., Andersson, U. B., Bauer, T. E., Wanhainen, C., Martinsson, O., Nordin, R., and Andersson, J. B. H.: Timing of plutonism in the Gällivare area: Implications for Proterozoic crustal development in the northern Norrbotten mining district, Sweden, *Geol. Mag.*, 155, 1-26, 2017.
- Smith, M., Coppard, J., Herrington, R., and Stein, H.: The geology of the Rakkurijärvi Cu-(Au)-prospect, Norrbotten: A new iron oxide copper gold deposit in northern Sweden, *Econ. Geol.*, 102, 393-414, 2007.
- Stephens, M. B.: Introduction to the lithotectonic framework of Sweden and organization of this Memoir, in: *Sweden: Lithotectonic Framework, Tectonic Evolution and Mineral Resources*, edited by: Stephens, M. B., and Bergman Weihed, J., *Geol. Soc. of London*, *Memoirs of the Geological Society of London*, 1-15, 2020.
- Westhues, A., Hanchar, J. M., Whitehouse, M. J., and Martinsson, O.: New constraints on the timing of host rock emplacement, hydrothermal alteration and iron oxide-apatite mineralization in the Kiruna district, Norrbotten, Sweden, *Econ. Geol.*, 111, 1595-1618, 2016.